# Conserved Folding in Retroviral Proteases: Crystal Structure of a Synthetic HIV-1 Protease

Alexander Wlodawer, Maria Miller, Mariusz Jaskólski,*
Bangalore K. Sathyanarayana, Eric Baldwin, Irene T. Weber, Linda M. Selk,
Leigh Clawson, Jens Schneider, Stephen B. H. Kent†

The rational design of drugs that can inhibit the action of viral proteases depends on obtaining accurate structures of these enzymes. The crystal structure of chemically synthesized HIV-1 protease has been determined at 2.8 angstrom resolution (R factor of 0.184) with the use of a model based on the Rous sarcoma virus protease structure. In this enzymatically active protein, the cysteines were replaced by $\alpha$-amino-$n$-butyric acid, a nongenetically coded amino acid. This structure, in which all 99 amino acids were located, differs in several important details from that reported previously by others. The interface between the identical subunits forming the active protease dimer is composed of four well-ordered $\beta$ strands from both the amino and carboxyl termini and residues 86 to 94 have a helical conformation. The observed arrangement of the dimer interface suggests possible designs for dimerization inhibitors.

THE MAJOR STRUCTURAL PROTEINS AND ENZYMES ESSENtial for replication of retroviruses, including the human immunodeficiency virus (HIV), are produced as high molecular weight polyproteins. The polyproteins are cleaved by a viral protease (PR) to give the mature structural proteins and enzymes, including the viral protease itself. The HIV-1 protease (1) is essential for the replication of infective virus (2), and is therefore an attractive target for the design of specific inhibitors as potential antiviral therapeutics.

The HIV-1 protease has been shown to belong to the class of aspartic proteases based on a variety of criteria, including distant sequence homology with cellular proteases (3, 4), inhibition by pepstatin A (5–9), and by mutational analysis of the active site Asp$^{25}$ (2, 7, 10, 11). The enzyme expressed in bacteria behaves as a dimer (8, 12). Recently, the crystal structures of the proteases from the Rous sarcoma virus (RSV) (13) and from HIV-1 (1) have been determined. Basically similar, these homologous molecules are

symmetric dimers with active sites resembling those in pepsin-like proteases (14). However, significant differences in main chain connectivity and secondary structure were observed between the reported crystallographic structures of these two homologous retroviral proteases. Particularly disturbing were the drastic differences in the topology of the dimer interface regions (15).

This puzzling disparity between the structures reported for the RSV and HIV-1 proteases was reinforced by a model of HIV-1 PR based on the crystal structure of RSV PR, proposed by Weber et al. (16). The model showed that the HIV-1 PR residues could be accommodated in a conformation almost identical to that of the RSV PR. Most of the differences between the RSV PR and the smaller HIV-1 PR molecule (124 amino acids versus 99 per monomer) were limited to contiguous regions located in two surface loops, and the core regions of the two structures were similar.

(H)-P$^1$ Q I T L W Q R P L$^{10}$ V T I [R] I G G Q L K$^{20}$

E$^{21}$ A L L D T G A D D$^{30}$ T V L E E M N L P G$^{40}$

[K]$^{41}$ W K P K M I G G I$^{50}$ G G F I K V R Q Y D$^{60}$

Q$^{61}$ I [P][V] E I [Aba] G H K$^{70}$ A I G T V L V G P T$^{80}$

P$^{81}$ V N I I G R N L L$^{90}$ T Q I G [Aba] T L N F$^{99}$-(OH)

**Fig. 1.** Amino acid sequence of [Aba$^{67,95}$]HIV-1 protease (SF2 isolate) (37). The residues that differ from the NY5 isolate (1) are boxed (replacements are R, K; K, R; P, L; and V, I). L-$\alpha$-Amino-$n$-butyric acid (Aba) was used in place of the two Cys residues, effectively substituting a methyl for the thiol group in the Cys side chain, to reduce synthetic difficulties associated with Cys deprotection and to ease product handling (17).

**Table 1.** Heavy atom parameters after lack-of-closure refinement, including anomalous scattering data. Mean figure of merit for 1692 observations was 0.76. The uranyl derivative (3 Å resolution) was obtained by soaking crystals for 16 hours in 1 m$M$ uranyl acetate in a sodium acetate buffer, $p$H 5.8, and the platinum derivative (4 Å resolution) by soaking in 0.05 m$M$ K$_2$PtCNS in the synthetic mother liquor. The uranyl ion is in the active site of the dimer, as is the case for RSV PR crystals, whereas platinum binds to the side chain of Met$^{46}$. Occupancy is in arbitrary units. The ($R_c$) is defined as Cullis R factor = $(\Sigma|F_{h(obs)} - F_{h(calc)}|)/\Sigma F_{h(obs)}$.

| Deriva-tive | Occu-pancy | $x$ | $y$ | $z$ | $B$ (Å$^2$) | $R_c$ |
|---|---|---|---|---|---|---|
| Uranyl | 1.3 | 0.848 | 0.848 | 0.000 | 38.1 | 0.34 |
| Platinum | 0.6 | 0.226 | 0.994 | −0.134 | 33.6 | 0.61 |

A. Wlodawer, M. Miller, M. Jaskólski, B. K. Sathyanarayana, E. Baldwin, and I. T. Weber are at the Crystallography Laboratory, NCI–Frederick Cancer Research Facility, BRI–Basic Research Program, P.O. Box B, Frederick, MD 21701. L. M. Selk, L. Clawson, J. Schneider, and S. B. H. Kent are at the Division of Biology, 147-75, California Institute of Technology, Pasadena, CA 91125.

*On leave from A. Mickiewicz University, Faculty of Chemistry, Poznań, Poland.
†Present address: Graduate School of Science and Technology, Bond University, Queensland, Australia 4229.

To resolve these discrepancies, we sought to independently determine the structure of the HIV-1 PR. In addition, no side chain locations were reported by Navia et al. (1). A molecular structure of the HIV-1 PR including side chain locations would be valuable for the understanding of the molecular origins of substrate specificity and for the rational design of inhibitors.

**Chemical synthesis and crystallization of [Aba67,95]HIV-1 protease.** The enzyme used in our study was prepared by total chemical synthesis (5, 17–20). The target amino acid sequence is shown in Fig. 1. The resulting enzyme preparation was homogeneous by reversed-phase high-performance liquid chromatography (HPLC) and SDS–polyacrylamide gel electrophoresis, and had the correct covalent structure, as determined by mass spectrometric peptide mapping. The synthetic enzyme had the specific proteolytic activity characteristic of the HIV-1 protease and had a turnover number comparable to that reported by Darke et al. for the enzyme derived from bacterial expression (21, 22).

Single crystals of HIV-1 PR were grown by a modification of the method described by McKeever et al. (23) and were isomorphous with those obtained by them (tetragonal space group $P4_12_12$, unit-cell parameters $a = 50.24$ Å, $c = 106.56$ Å) (24).

**Solution of the crystal structure.** For data collection, two native crystals were mounted in capillaries in a synthetic mother liquor that consisted of 250 mM NaCl in 50 mM sodium cacodylate buffer, pH 7.0. X-ray diffraction data were collected with a Siemens electronic area detector (25). The number of reflections measured to 2.8 Å resolution was 26,037, which reduced to 3,225 unique data, of which 2,614 were considered observed [$I > 1.5\sigma(I)$]. Diffraction data for uranyl and platinum heavy atom derivatives were collected

from one crystal each, to the resolution of 3 Å and 4 Å, respectively (Table 1).

The crystal structure was solved first by molecular replacement and then confirmed by the multiple isomorphous replacement (MIR) method. The molecular replacement method used the HIV-1 protease model constructed by Weber et al. (16) based on the known structure of the RSV PR (13). The asymmetric unit of the HIV-1 PR crystals contains a single protein subunit, and the protease dimer is generated by the operation of the crystallographic twofold axis along the diagonal direction in the tetragonal unit cell. The model of the HIV-1 PR dimer was initially placed in the unit cell with its twofold axis along [110]. The program package MERLOT (26) was then used to rotate an origin-centered monomer of this partially oriented model by 180° around the [110] direction to find the orientation consistent with the Patterson function of the diffraction data. The solution (with the highest peak at $4.3\sigma$) clearly indicated the correct orientation of the model in the unit cell.

For the translation search, the space group enantiomorph reported previously (1) was assumed. The results of that search gave a clear indication of the $x$ and $y$ translations but no consistent solution for the $z$ translation. The placement of the monomer along the $c$-axis was deduced by finding that $z$ translation at which the proper protease dimer could be generated by the crystallographic twofold axis. The dimer generated in this way is consistent with the reported Pb position at the active site (1). Rigid body refinement performed with the program CORELS (27), with the flap included as a separate domain, converged at an $R$ factor of 0.465, and a correlation coefficient of 0.46. The model was further refined with the molecular dynamics program, X-PLOR (28), followed by restrained
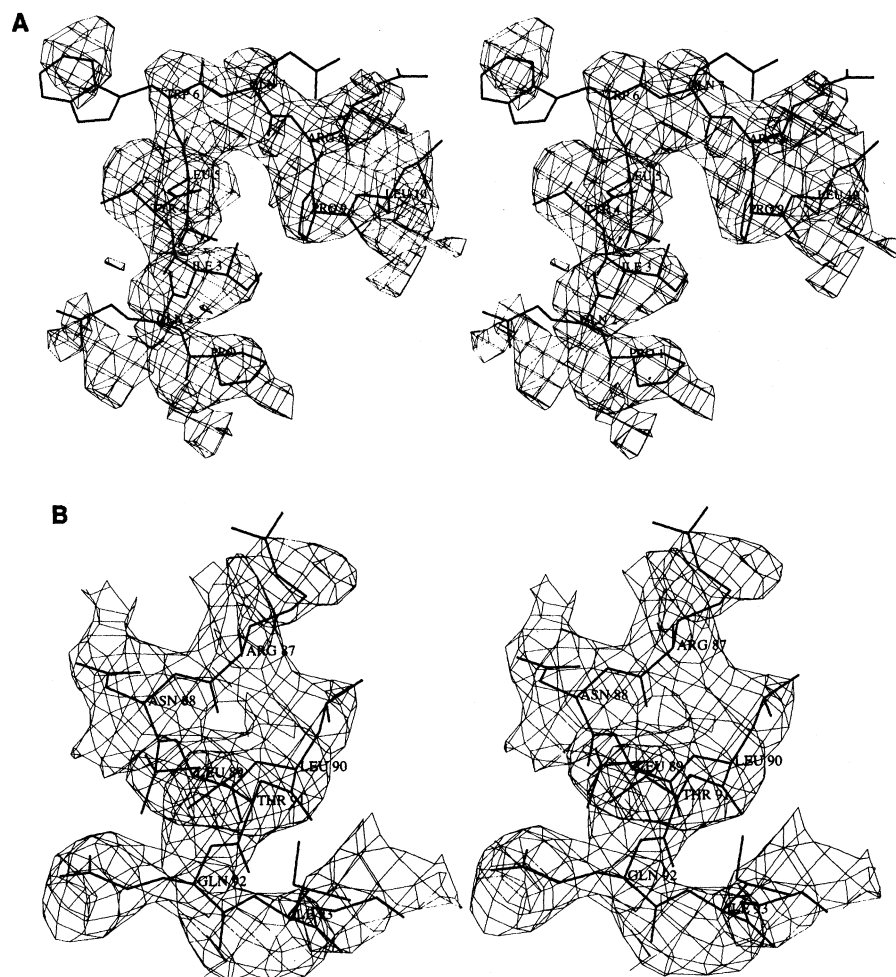
**Fig. 2.** Stereo views of the MIR electron density map that was improved by solvent flattening (31). Contour level is $1\sigma$. (**A**) Residues 1 to 10 (final refined coordinates) superimposed on the electron density. (**B**) Residues 86 to 94, which were found in a helical conformation [the atomic coordinates were taken directly from the model predicted by Weber et al. (16) and fit the electron density before any refinement].
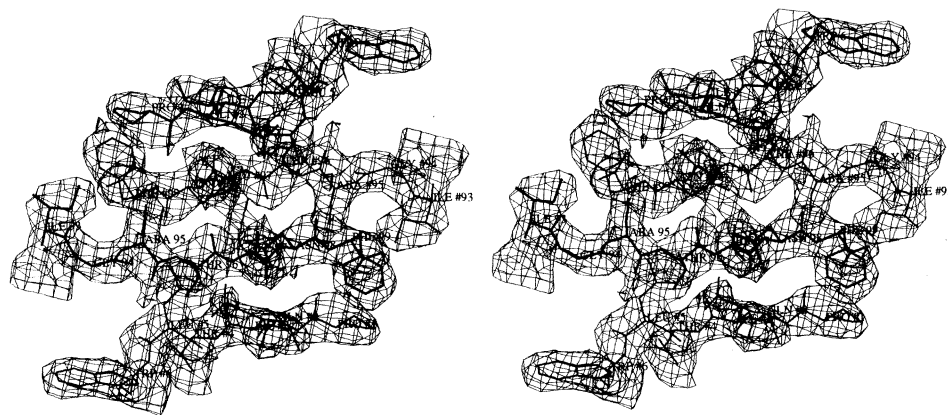
**Fig. 3.** A stereo view of the electron density and of the final atomic model at the dimer interface in the HIV-1 protease. Residues 1 to 5 and 93 to 99 are shown for both subunits, and those marked # correspond to the crystallographically related molecule. This $2F_o - F_c$ electron density map was calculated after refinement and was contoured at $1\sigma$ level. This arrangement of the dimer interface is in agreement with the Hg sites in the heavy atom derivatives of HIV-1 PR (*1*), since one of the reported sites is close to the tip of residue 95 (Cys in the original structure, Aba here).

least squares minimization, PROLSQ (*29*), and manual rebuilding into $2F_o - F_c$ Fourier maps with FRODO (*30*).

While the refinement was under way, diffraction data for two heavy atom derivatives were collected (Table 1). The solvent-flattening method of Wang (*31*) was applied to the MIR solution. The resulting map was used as an aid in further stages of manual rebuilding, particularly in the turn around residue 6 and in the tip of the flap. Individual, tightly restrained temperature factors were used in the refinement, but no water molecules were included. The final $R$ factor after the refinement as described above is 0.184 with good geometry (deviations from ideal bond lengths of 0.026 Å) and with an average $B$ of 16.9 Å$^2$.

**Electron density maps.** The electron density map calculated with MIR phases improved by solvent flattening is of medium quality, most probably because of limited phase information provided by the uranyl derivative (for which the heavy atom is in a special position). Although most of the chain was found in contiguous density, a number of breaks were present and chain tracing would have been much more difficult in the absence of the information provided by the molecular replacement solution (Fig. 2A). This MIR electron density map was, however, in good agreement with the partially refined model, and thus independently verified the structure derived by molecular replacement. In particular, the positions of the helix (Fig. 2B) and of the flap were clearly indicated by continuous density. The final $2F_o - F_c$ map calculated upon completion of the refinement is excellent (Fig. 3), with no breaks at $1\sigma$ level in the density corresponding to the main chain. The electron densities for the two unnatural amino acids confirm the replacement of the thiol groups of cysteines by methyl groups. This position concerns the native fold of the synthetic PR (Fig. 3). Even at the limited resolution of 2.8 Å, clear solvent density was visible. In particular, a water molecule residing between the two symmetry-related side chains of Asp$^{25}$ could be seen (Fig. 4). Such density has been reported for all uncomplexed aspartic proteases (*14*). Although this and other solvent molecules could be seen, they were not included in the refinement.

**Description of the structure.** The general topology of the HIV-1 PR molecule (Figs. 5 and 6) is similar to that of a single domain in pepsin-like aspartic proteases (*32*). The main difference is in the interface region where the two HIV-1 PR monomers have significantly shorter NH$_2$- and COOH-terminal strands that interact to produce a dimer whose structure and properties are similar to those of the two-domain, pepsin-like enzymes. The NH$_2$-terminal β strand a (residues 1 to 4) forms the outer part of the interface β sheet. The b β strand (9 to 15) continues through a turn into the c β chain, which terminates at the active site triad (25 to 27). Following the active-site loop is the d β chain with residues 30 to 35. In pepsin-like proteases, the d chain is followed by the h helix which in

RSV PR is reduced to a short and distorted segment. In HIV-1 PR this fragment is even more distorted and has the form of a broad loop (36 to 42). The second half of the molecule has a topology related to that described above by the approximate intramolecular twofold axis (corresponding substructures indicated by primed labels). Residues 43 to 49 form the a' β strand which, as in pepsin-like proteases, belongs to the flap. The other strand in the flap (52 to 58) forms a part of the long b' β chain (52 to 66). The flap is most probably stabilized by a pair of hydrogen bonds between main chain atoms of residue 51, located at the tip of the flap, and its symmetry mate in the crystallographic dimer. The c' β chain comprises residues 69 to 78 and after a loop at 79 to 82 continues as chain d' (83 to 85) which leads directly to the well-defined helix h' (86 to 94). The hydrogen bonding pattern within this helix is intermediate between the α helix and the $3_{10}$ helix. Helix h' is followed by a straight COOH-terminal β strand (95 to 99), which can be designated as q, in a way analogous to RSV PR. In contrast, pepsin-like aspartic proteases have a double-stranded β sheet here. This COOH-terminal region forms the inner part of the intra-dimer interface. Four of the β strands in the molecular core are organized into a ψ-shaped sheet characteristic of all aspartic proteases. One of the ψ letters comprises chains c (23 to 25), d, and d' and the other is made up of c' (76 to 78), d', and d.

The active-site triad (Asp$^{25}$-Thr$^{26}$-Gly$^{27}$) is located in a loop whose structure is stabilized by a network of hydrogen bonds characteristic of aspartic proteases. The symmetry-related Asp$^{25}$ carboxylic groups from the two loops composing the active site are nearly coplanar and show a close contact involving their Oδ1 atoms (Fig. 4). In addition, the two active-site loops are linked by the "fireman's grip" in which each Thr (the middle residue in the active-site triad) accepts a hydrogen bond from the Thr amide group in the other loop and donates a hydrogen bond to the carbonyl O atom in the residue preceding the catalytic triad on the other strand. The structure of each individual loop is reinforced by a hydrogen bond between Oδ1 of the aspartate and the NH group of the Gly$^{27}$, the last residue in the triad. In all pepsin-like enzymes the residue immediately following the active-site triad has a hydroxyl group (the only exception is one domain of human renin, which has alanine in this position), which usually forms a hydrogen bond with the side chain of the catalytic Asp on the same strand. This result is in contrast with retroviral proteases, which invariably have Ala in this position, so that no such hydrogen bonding is possible.

**Comparison with other aspartic proteases.** The final model of the HIV-1 PR was compared with the structure of RSV PR, which has been refined to $R = 0.148$ at 2 Å resolution (*33*). The agreement is very close, with a root-mean-square (rms) deviation of 1.5 Å for 86 common Cα atoms in one subunit. With minor exceptions, the corresponding Cα atoms follow closely the sequence alignment

proposed previously (16). Detailed comparisons, however, showed that deletions of several residues from the RSV PR sequence, in addition to those previously proposed, were necessary to properly align it with the HIV-1 PR. They include residues 7, 8, 48, 49, and 93 (RSV numbering). Since the structure of the flap region was not seen in the RSV protease (13), no correction in the alignment is possible for that region.

Following the previous comparisons of the structure of RSV PR and pepsin-like proteases (34), the present structure of HIV-1 PR has been compared with both domains of rhizopuspepsin (35). Contrary to previous observations (1), we found no difference between the fit to the C- and N-domains. For the N-domain of rhizopuspepsin, we could superimpose 57 Cα pairs (more than one-half of all residues in HIV-1 PR) to an rms deviation of 1.4 Å, whereas 56 Cα pairs in the C-domain superimposed within the same limits. It must be stressed that different elements of the secondary structure in each domain are responsible for some of these alignments.

Comparisons of all atoms in the active sites (the catalytic triad flanked by four residues on each side), showed that 126 atom pairs superimposed with an rms deviation of 0.57 Å between HIV-1 PR and RSV PR, whereas the optimum superposition between HIV-1 PR and rhizopuspepsin included 88 pairs deviating by 0.59 Å. These results show close similarity between the retroviral enzymes, whereas the latter comparison agrees with the numbers reported for the comparison of RSV PR and pepsin-like proteases (34).

**Comparison with the previously determined HIV-1 PR structure.** We can make only general comparisons with the previously published structure (1), since we had no direct access to the atomic coordinates resulting from that work. Two major questions must be addressed. First, that structure had no indication of a helix, although a helix is present in the RSV PR structure (13) and belongs to a region that is highly conserved between the cellular and viral proteases, as shown on the basis of sequence alignments and structural similarities of RSV PR and pepsin (34). Second, the NH2-

and COOH-terminal regions were arranged differently from the topology observed at the dimer interface in RSV PR. These results were difficult to understand, considering the sequence alignments and structural comparisons which suggested close similarity between HIV-1 and RSV proteases.

The current work resolves these difficulties and corrects the previously reported structure. A helix is evident in both the MIR electron density map (Fig. 2) and in the final $2F_o - F_c$ maps. This helix (residues 86 to 94) is in close agreement with that in the model structure derived from the RSV protease (16) and is consistent with the sequence and structural similarities of viral and pepsin-like proteases (34). The length of the helix is in excellent agreement with the presence of 6.5 percent helical structure in HIV-1 PR, as determined by circular dichroism (8).

Residues 1 to 5 at the NH2-terminus, which were previously reported to be disordered (1), are clearly visible in the present electron density maps (Fig. 3). The NH2- and COOH-termini are arranged into a four-stranded antiparallel β sheet (Figs. 4 and 6). This β sheet, composed of alternate strands from the termini of each subunit in the dimer, is similar to that present in the RSV PR (13). In both cases there are several hydrogen-bond interactions that presumably stabilize this β sheet conformation. Since the NH2-terminus is held tightly in place by an ionic interaction with the COOH-terminus of the other subunit, this arrangement of the termini at the dimer interface is inconsistent with the intramolecular mechanism proposed for the release of the HIV-1 PR from the precursor polyprotein (1), in which the disordered NH2-terminus was assumed to be cleaved after it folded back into the active site.
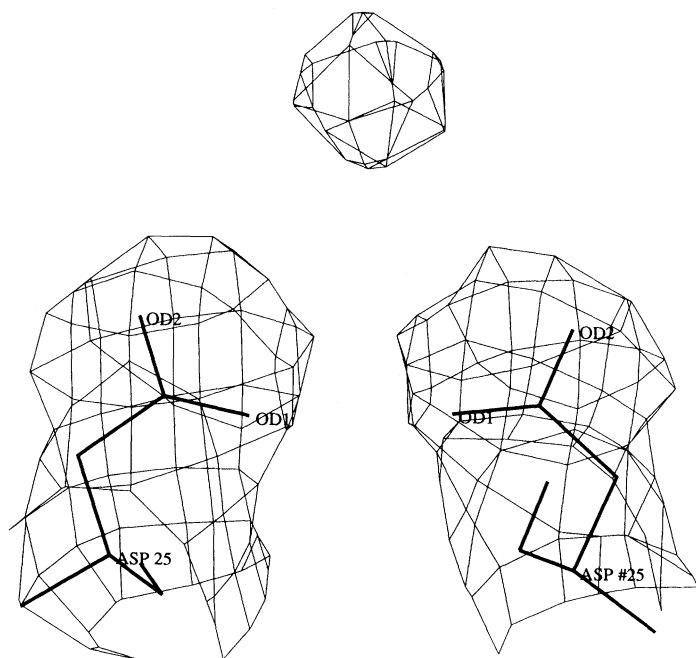


**Fig. 4.** Active-site electron density ($2F_o - F_c$ Fourier synthesis, contour level 0.85σ) showing a density for the water which is found in a similar position in all native structures of aspartic proteases. The distance of this water from the carboxylate O atoms is slightly greater than expected, but this would probably change upon refinement.
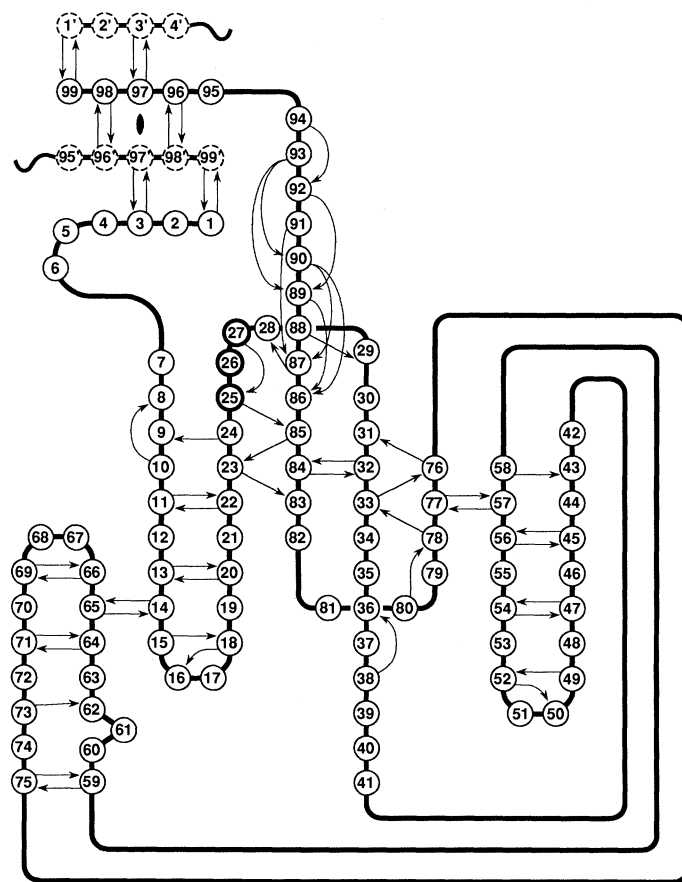


**Fig. 5.** Diagram of the secondary structure of the HIV-1 protease. Main chain NH⋯O hydrogen bonds are indicated by arrows. The active site (Asp-Thr-Gly) is marked by thicker circles, and the broken circles correspond to residues from the symmetry-related molecule in the dimer interface.

**Fig. 6.** A view of the Cα backbone tracing of the fully refined model of the HIV-1 protease dimer, in an orientation emphasizing the interactions in the dimer interface. The full set of atomic parameters for this model, including both the main chain and side chain atoms, has been deposited with the Brookhaven Protein Data Bank (set 3HVP).

We suggest that only intermolecular catalysis is responsible for the release of the protease in both RSV and HIV-1.

**Comparison with previously proposed models of HIV-1 PR.** This experimentally determined structure of HIV-1 PR has been compared with the results of the two previous modeling efforts. The superposition of the Cα atoms onto the atomic coordinates of Pearl and Taylor (4) yielded an rms deviation of 2.6 Å for 87 atom pairs. In a number of places the residues were shifted by one or two positions, but the general agreement was remarkably good, considering that the model was based on distant similarities to nonviral, pepsin-like proteases.

A comparison with the model of Weber et al. (16), which was based on the closely related RSV protease, yielded an rms deviation of 1.3 Å for 82 Cα atoms. In this comparison residues 1 to 6 in the refined model are shifted by two positions toward the NH₂-terminus. Deviations along the flap (residues 43 to 58) were as large as 7 Å because the flat was originally modeled in a position close to the active site as observed in a rhizopuspepsin-inhibitor complex (35). The location of the active site and substrate binding residues, however, was predicted quite accurately in the model of Weber et al. (16). In particular, the significance of mutations at $Arg^{87}$ and $Asn^{88}$ was correctly understood from that model, whereas it was not obvious from the structure reported by Navia et al. (1). $Arg^{87}$ is located in the helix and forms an ionic interaction with $Asp^{29}$ near the catalytic site. This is consistent with the results of mutations of $Arg^{87}$ or $Asn^{88}$ that produce inactive protease (36). Detailed modeling of inhibitor complexes based on our structure should help explain the observed differences in specificity between the RSV and HIV proteases, and can be used to design better inhibitors.

**Potential applications.** Our results confirm that a number of conserved features of the three-dimensional structure of aspartic proteases are also conserved in the retroviral enzymes and reinforces the notion that modeling of unknown structures based on the structures of related proteins can often give accurate results. A chemically synthesized protein can crystallize isomorphously with the protein obtained from living cells and can fold correctly without being exposed to a ribosome. The coordinates of the HIV-1 PR provided in this study will be useful in rational drug design. The information on side chain positions should allow more systematic investigations of the mechanism of this important enzyme to be made, especially with respect to design of specific inhibitors for use as potential therapeutics against AIDS. Furthermore, drugs could be designed including drugs that interfere with the dimerization and hence inactivate the enzyme through an alternative mechanism. It should be noted that one of the terminal strands contains a free Cys residue, thus suggesting a site of covalent attachment for a compound designed along these lines.

**REFERENCES AND NOTES**

1. M. A. Navia et al., Nature 337, 615 (1989).
2. N. E. Kohl et al., Proc. Natl. Acad. Sci. U.S.A. 85, 4686 (1988).
3. H. Toh, M. Ono, K. Saigo, T. Miyata, Nature 315, 691 (1985).
4. L. Pearl and W. Taylor, ibid. 329, 351 (1987).
5. J. Schneider and S. B. H. Kent, Cell 54, 363 (1988).
6. J. Hansen, S. Billich, T. Schulze, S. Sukrow, K. Moelling, EMBO J. 7, 1785 (1988).
7. S. Seelmeier, H. Schmidt, V. Turk, K. von der Helm, Proc. Natl. Acad. Sci. U.S.A. 85, 6612 (1988).
8. P. L. Darke et al., J. Biol. Chem. 264, 2307 (1989).
9. A. D. Richards, R. Roberts, B. M. Dunn, M. C. Graves, J. Kay, FEBS Lett. 247, 113 (1989).
10. S. F. J. Le Grice et al., EMBO J. 7, 2547 (1988).
11. D. D. Loeb, C. A. Hutchison, M. H. Edgell, W. G. Farmerie, R. Swanstrom, J. Virol. 63, 111 (1989).
12. T. D. Meek et al., Proc. Natl. Acad. Sci. U.S.A. 86, 1841 (1989).
13. M. Miller, M. Jaskólski, J. K. M. Rao, J. Leis, A. Wlodawer, Nature 337, 576 (1989).
14. M. N. G. James and A. R. Sielecki, in Biological Macromolecules and Assemblies, F. A. Jurnak and A. McPherson, Eds. (Wiley, New York, 1987), pp. 413–482.
15. T. L. Blundell and L. Pearl, Nature 337, 596 (1989).
16. I. T. Weber et al., Science 243, 928 (1989).
17. The following side chain protection was used: Asp and Glu, benzyl-protected carboxyl group (OBz); Asn, Gln, and Met, unprotected; Lys, dichlorobenzyloxy-

carbonyl (2ClZ); Trp, formyl; His, 2, 4-dinitrophenyl (DNP); Arg, tosyl; Thr, benzyl, and Tyr, bromobenzyloxycarbonyl (BrZ). Machine-assisted assembly of the protected 99-residue peptide chain was carried out by stepwise addition of amino acids to the resin-bound carboxyl terminal residue (18), and took 3.3 days. Protection of Nα side chains with tert-butyloxycarbonyl (Nα Boc chemistry) was used, in combination with highly optimized synthetic protocols specifically developed for the preparation of long polypeptide chains (19). Side chain protecting groups were removed and the peptide chain cleaved from the resin with a modified $S_N2$–$S_N1$ treatment with strong acid (20) after prior removal of the $N^\alpha$-Boc, His (DNP), and Trp (formyl) groups to prevent side reactions. The resulting crude polypeptide product was dissolved in 6M guanidine·HCl (GuHCl) buffered to pH 7.0 and was worked up by gel filtration (G50, in 6M GuHCl), followed by semipreparative reversed-phase HPLC (0.1 percent trifluroacetic acid versus acetonitrile). The purified polypeptide was dissolved in 6M GuHCl, 25 mM phosphate, pH 7.0 at a concentration of 200 μg/ml and was folded by slow dialysis versus decreasing concentrations of GuHCl, to the final 25 mM phosphate-buffered to pH 7.0, 10 percent glycerol, and concentrated in a Centriprep 10/ Centricon 10 to ~3 mg/ml.

18. R. B. Merrifield, J. Am. Chem. Soc. 85, 2149 (1963).
19. S. B. H. Kent, Annu. Rev. Biochem. 57, 957 (1988).
20. J. P. Tam, W. F. Heath, R. B. Merrifield, J. Am. Chem. Soc. 105, 6442 (1983); ibid. 108, 5242 (1986).
21. P. L. Darke et al., Biochem. Biophys. Res. Commun. 156, 297 (1988).
22. The soluble, folded synthetic enzyme had a turnover number of 300 min⁻¹, at pH 6.0 with a 12-residue synthetic peptide analog of the p17/p24 (MA/CA) Tyr-Pro cleavage site, comparable to that (240 min⁻¹) reported by Darke et al. (8) on a related substrate under slightly different conditions.
23. B. M. McKeever et al., J. Biol. Chem. 264, 1919 (1989).
24. The protein sample was dialyzed against 50 mM sodium cacodylate buffer, pH 7.0, 0.1M NaCl and subsequently concentrated slightly by dialyzing against 12.5 percent (w/v) polyethylene glycol 14,000 in the same buffer to compensate for the increase in volume during removal of glycerol. Droplets (10 to 25 μl) were sealed over 1-ml reservoirs containing 10 to 30 percent ammonium sulfate. The total amount of refolded protein used in this study was ~1 mg. Crystals were shaped as tetragonal bipyramids and usually appeared after 5 to 7 days and reached their maximum size (0.35 mm) within another week.
25. A. J. Howard et al., J. Appl. Crystallogr. 20, 383 (1987).
26. P. M. D. Fitzgerald, ibid. 21, 53 (1988).
27. J. L. Sussman, Methods Enzymol. 115, 271 (1985).
28. A. T. Brünger, J. Kuriyan, M. Karplus, Science 235, 458 (1987).
29. W. A. Hendrickson, Methods Enzymol. 115, 252 (1985).
30. A. T. Jones, J. Appl. Crystallogr. 11, 268 (1978).
31. B. C. Wang, Methods Enzymol. 115, 90 (1985).
32. T. L. Blundell, J. Jenkins, L. Pearl, T. Sewell, V. Pedersen, in Aspartic Proteinases and Their Inhibitors, V. Kostka, Ed. (de Gruyter, Berlin, 1985), pp. 151–161.
33. M. Jaskólski, M. Miller, J. K. M. Rao, J. Leis, A. Wlodawer, unpublished results.
34. J. Erickson, J. K. M. Rao, C. Abad-Zapatero, A. Wlodawer, unpublished results.
35. K. Suguna, E. A. Padlan, C. W. Smith, W. D. Carlson, D. R. Davies, Proc. Natl. Acad. Sci. U.S.A. 84, 7009 (1987).
36. J. M. Louis, C. A. Dale Smith, E. M. Wondrak, P. T. Mora, S. Oroszlan, unpublished results.
37. Abbreviations for the amino acid residues are: A, Ala; C, Cys; D, Asp; E, Glu; F, Phe; G, Gly; H, His; I, Ile; K, Lys; L, Leu; M, Met; N, Asn; P, Pro; Q, Gln; R, Arg; S, Ser; T, Thr; V, Val; W, Trp; and Y, Tyr.
38. We thank the Advanced Scientific Computing Laboratory, FCRF, for computer time on their CRAY X-MP. Sponsored in part by the National Cancer Institute, DHHS, under contract N01-CO-74101 with BRI, and in part by funds from the NSF Biological Instrumentation Division to S.B.H.K.

---

being sought by one federal program alone for the purpose of reducing exposure to low levels of radiation and chemical wastes on the basis of largely hypothetical health risks (16).

---

### REFERENCES AND NOTES

1. C. Congdon, Health Phys. 52, 593 (1987).
2. L. Feinendegen, H. Muhlensiepen, V. Bond, C. Sondhaus, ibid., p. 663.
3. S. Wolff et al., Int. J. Radiat. Biol. 53, 39 (1988).
4. H. Tuschl et al., Radiat. Res. 81, 1 (1980).
5. S. Kondo, Int. J. Radiat. Biol. 53, 95 (1988).
6. J. Fabrikant, Health Phys. 52, 561 (1987).
7. S. Liu, ibid., p. 579.
8. S. James and T. Makinodan, Int. J. Radiat. Biol. 53, 137 (1988).
9. High Background Radiation Research Group, China, Science, 209, 877 (1980).
10. W. J. Schull, M. Otake, J. V. Neel, ibid., 213, 1220 (1981).
11. B. Strauss, ISI Atlas of Science: Biochemistry (Institute for Scientific Information, Philadelphia, PA, 1988), vol. 1, pp. 1–5.
12. H. Boxenbaum, P. Neafsey, D. Fournier, Drug Metab. Rev. 19, 195 (1988).
13. T. Luckey, Hormesis With Ionizing Radiation (CRC Press, Boca Raton, FL, 1980).
14. Collected papers from the Conference on Radiation Hormesis, held at Oakland, CA, 14 to 16 August 1985, Health Phys. 52, 517 (1987).
15. Proceedings of the Workshop on Low Dose Radiation and the Immune System, 5 to 8 May 1987, Dreieich-Frankfurt, Federal Republic of Germany, Int. J. Radiat. Biol. 53, 1 (1988).
16. U.S. Department of Energy, Environment, Safety, and Health Needs of the U.S. Department of Energy, vol. 1, Assessment of Needs (Rep. DOE/EH-0079-vol. 1, U.S. Department of Energy, Washington, DC, 1988).

---

phocytes exposed to 1 cGy of x-rays shows that certain proteins are absent in all control cultures, but are reproducibly present in all irradiated cultures. These proteins represent excellent candidates for being the induced enzymes needed for the repair of the cytogenetic damage.

Nevertheless, the fact that a protein (enzyme) involved in repair can be induced by very low doses of radiation does not necessarily mean that these doses are in and of themselves "good" or hormetic. Several new proteins were found to have been induced, which indicates that the metabolism of the cells had been changed. Some of these proteins might have a metabolic effect of their own, and could possibly lead to a cascade effect whereby subsequent metabolic steps unrelated to the induced repair would be altered. To call this beneficial would be premature, indeed.

---

### REFERENCES AND NOTES

1. National Research Council, Advisory Committee on the Biological Effects of Ionizing Radiations, "The effects on populations of exposure to low levels of ionizing radiations" (report, National Research Council, Washington, DC, 1972).
2. K. Sax, Am. J. Botany 42 (no. 4), 360 (1955).
3. J. Cairns, J. Overbaugh, S. Miller, Nature 335, 142 (1988).
4. F. W. Stahl, ibid., p. 112.
5. G. Olivieri, J. Bodycote, S. Wolff, Science 223, 594 (1984).
6. J. K. Wiencke, V. Afzal, G. Olivieri, S. Wolff, Mutagenesis 1, 375 (1986).
7. J. D. Shadley and S. Wolff, ibid. 2, 95 (1987).
8. J. D. Shadley, V. Afzal, S. Wolff, Radiat. Res. 111, 511 (1987).
9. S. Wolff, V. Afzal, J. K. Wiencke, G. Olivieri, A. Michaeli, Int. J. Radiat. Biol. 53, 39 (1988).
10. S. Wolff, J. K. Wiencke, V. Afzal, J. Youngblom, F. Cortés, Low Dose Radiation: Biological Bases of Risk Assessment (Taylor & Francis, London, in press).
11. T. Ikushima, Mutation Res. 180, 215 (1987).
12. Supported by the Office of Health and Environmental Research, U.S. Department of Energy, contract no. DE-AC03-76-SF01012.